Supplementary text S1

Morphological and phenotypic diversity among end point isolates

88 end point clones isolated from the Replicate 1 population and 82 from Replicate 2 showed dramatic variations in morphology and phenotypic traits. The most noticeable difference was in the colony size, texture and color of the individual isolates (Fig. S1(a)). Colonies ranged from large to small, dry to mucoid and translucent to deep blue-green. Preliminary MIC tests showed that isolates ranged from being completely susceptible to completely colistin resistant (Fig. S1(b)). MICs of other antibiotics were tested to determine cross sensitivities. Some isolates that had acquired colistin resistance showed cross-sensitivity to antibiotics like rifampicin, piperacillin, imipenem, cefotaxime and chloramphenicol. However, this was not consistent among all colistin resistant isolates and hence, could not be considered as a phenomenon associated with colistin resistance. Analysis of growth rates of some isolates showed that the isolates also varied in terms of their overall fitness in the absence of colistin (Fig. 6).

Genetic diversity in PAO1 and dynamics of the Pf4 phage encoded region during adaptation

A low level of genetic diversity was seen in the initial population of PAO1 growing in the bioreactor in the absence of colistin with mutations at low frequencies (typically less than 10%) distributed throughout the genome (Fig. 2). A part of the ancestor colony that was used to inoculate the vessel was grown separately in a glass tube and genomic DNA was extracted from this sample for whole genome sequencing. When this ancestor was run using the polymorphism

command on Breseq (1) and compared to the reference genome, the same level of genetic diversity was also seen in the ancestor, suggesting that this is an inherent phenomenon in *Pseudomonas aeruginosa* PAO1 and is not stimulated by growth in the bioreactor.

In contrast with the low level diversity seen in the majority of the PAO1 genome, the Pf4 phage encoded region spanning positions 7.8×10^5 to 8×10^5 bp on the chromosome exhibited higher genetic variability and the mutations in this region reached approximately 50% frequency in the population under non-selective growth conditions (Day 1). When the population was exposed to the first sub-inhibitory dose of colistin (Day 2 for Replicates 1 and 2), a sudden collapse in the genetic diversity in the phage encoded region was observed (Fig. 2). This collapse was accompanied by the appearance of circularized phage particles in the bioreactor vessel. This became evident from the whole genome sequencing data of the polymorphic population from day 2 which showed a new junction that coincided with the circularization of the phage encoded DNA. The sequencing reads mapping to the phage encoded region on day 2 had more than 15-fold higher coverage than the reads mapping to the rest of the genome. Taken together, this suggested that the prophage had become lytic upon exposure to colistin and had formed superinfective Pf4 bacteriophage. The circularized phage had lost genes PA0715 (encoding a reverse transcriptase) and PA0716 (encoding the ATPase component of an ABC transporter). Identical observations were made in replicate PAO1 adaptation experiments. Fig. S2 (a) depicts the phage excision event. In contrast, while excision of the phage encoded region and junctions representing circular phage particles were observed in the population of cells evolving without the drug (no drug control experiment), they did not have the severe collapse in diversity in the phage encoded region that was observed during the first exposure to colistin on day 2 of

Replicates 1 and 2. The loss of diversity suggests that substantial stress was experienced by the population despite the very low sub-MIC concentration of colistin.

Consistent with these observations, the supernatant obtained after centrifugation of a sample of the day 2 population had lytic activity on a lawn of PAO1. Similar supernatant from day 1 of adaptation did not (Fig. S2 (b)). This lytic activity was also seen on days 13 and 25 of adaptation during Replicate 1 (Fig. S2 (b)) but the genomic variability in the phage encoded region that was lost on day 2 was restored by day 6 (Fig. 2). It has been suggested that an integrated prophage can represent a genetic burden to the host and thus, the prophage may risk accumulating mutations that render it defective unless it confers a selective advantage to the host (2). Although it is unclear why this phage encoded region presents such variability in DNA sequence, it can be hypothesized that mutations at low to intermediate frequency in the phage encoded region restrict the prophage from becoming lytic. It has been shown that biofilm growth and dispersal can induce mutations in Pf4, triggering its switch from lysogenic to lytic phase (3). Stressors inducing DNA damage as well as exposure of bacteria to sub-inhibitory concentrations of antibiotics have been shown to induce delysogenization and development of superinfective phage (4, 5). The prophage excision event coincided with the first exposure of PAO1 to sub-inhibitory concentration of colistin in this experiment. While superinfective phage can kill delysogenized PAO1, a portion of the PAO1 cells may still be lysogenic and immune to phage mediated killing which then re-populate the bioreactor after the phage bloom. Although the junction representing circularized phage is not detected in the genome sequences of populations from later days of evolution, the supernatants from these populations are still capable of lysing the PAO1 host (Fig. S2 (b) days 13 and 25) suggesting that the circularized replicative phage

persist in the vessel and may be biofilm associated since they are known to play a role in biofilm dispersal and stabilization (3, 6, 7).

Additional information on Fisher's Exact Test of end point isolates

Several genes cluster very close to the bottom left quadrant of the graph depicted in Fig. 4 in the main text. These genes were not commonly mutated and based on the Fisher's Exact test, were not statistically significant for being adaptive. These mutations were most likely the hitchhikers. Also noteworthy were two clusters of genes mutated in 20 to 60% of the end point isolates (Fig. 4). Once these genes were mapped on the phylogenetic trees to investigate their significance, it was clear that they grouped into specific branches of the tree. Six of the genes could be placed on the branch containing *fadD2* on the tree from Replicate 1. Nine of them could be placed on the branch containing *mutS* (9 bp deletion) on the tree from Replicate 2. The clustering of all the genes on one particular branch of the tree and their presence in susceptible as well as resistant end point isolates suggested that they were also most likely hitchhiker mutations. Several genes clustered in the top left quadrant of the graph (Fig. 4) but only some of them were identified as being significant to resistance by this test (highlighted in red in Fig. 4) This suggested that the criteria used in the Fisher's Test provided one useful method to screen mutations in a highly complex data set.

It should be noted that in cases where a very limited number of mutations in a gene are viable and can confer resistance, that gene may not be captured by this test using whole genome sequence data of end point isolates. However, if that mutation occurs independently and repeatedly in multiple replicate evolving populations, the mutation in each population accounts for a unique event and will be identified as significant by this test using metagenomic sequencing data of the daily populations. This further highlights the importance of collecting whole genome

sequencing information, not only of the end point isolates but also of replicate metagenomic evolving populations for identification of adaptive alleles.

Mutations acquired by *pmrB* during adaptation to colistin

16 unique mutations were identified in *pmrB* at ≥ 5% frequency in the population of PAO1 adapting to colistin. The transmembrane domains (spanning amino acids 15-37 and 161-183) of this sensor kinase (shown in Fig. 5) that form a 4 helical bundle in the dimeric sensor protein had acquired mutations L17P, L18P, Y33H, L162P, L167P and L170P. Interestingly, barring Y33H, all the mutations seen in the transmembrane regions were leucine to proline substitutions. Proline is not typically found in α-helices since it lacks the free N-H group needed to form an intrahelix hydrogen bond and favors a main chain kink in the helix, leading to destabilization (8, 9). PmrB is known to activate genes involved in cationic peptide resistance (10–12). We speculate that the leucine to proline mutations may alter the structure of the transmembrane region responsible for transducing signal to the kinase domain in a manner that either mimics or makes it easier to achieve activated state to increase phosphorylation of PmrA by the kinase domain of PmrB, thereby altering expressing of genes involved in CAP resistance. Supporting this suggestion is previous work showing that the lipid A profile of a colistin resistant strain having a L167P substitution in PmrB shows aminoarabinosylation of lipid A, which is a function of the PmrAB regulated *arn* operon and imparts resistance to CAPs (13).

The periplasmic domain (residues 38-160) that senses external stimuli (CAPs, in the case of PmrB) and transmits the signal to the transmembrane domain had mutations D47G, ΔD47, M48I and V136M. The intracellular signal transducing HAMP domain (found in histidine kinases, adenylate cyclases, methyltransferases and phosphodiesterases) spanning amino acids 184 to 238 had 1 mutation, V185A. 3 mutations within the dimerization and histidine

phosphotransfer domain (DHP) were identified: L243R, A248T and M292T. The C-terminal ATP binding domain had 2 mutations: A330P and F408L.

The ability of PmrB to acquire mutations in every single domain and remain active suggests that each of these mutations only modestly affect its activity and these subtle changes are enough to alter the expression of genes in the regulon of this two-component system sensor kinase and confer resistance. If only a modest change in protein function is sufficient for fitness then there are likely to be many point mutations capable of generating the required modest changes. Conversely, if a very large change in a physicochemical property is required such as a very large change in k_{cat}, there will be far fewer, if any, single mutations that can produce such a change. It has been shown that different *pmrB* mutants are capable of conferring different degrees of polymyxin resistance in *P. aeruginosa* and are capable of increasing transcription from the *arnB* promoter up to 32-fold (10). This supports previous observations that subtle changes in protein function can have large fitness effects favoring adaptation to antibiotic resistance (14, 15).

Protection offered by biofilm may explain susceptibility of some end point isolates

Although the final evolved populations were growing at $\geq$ 16 µg/ml colistin, a portion of the populations had remained colistin susceptible. Preliminary MIC tests of 88 end point clones isolated from the Replicate 1 population and 82 from Replicate 2 showed that 14% of selected isolates from Replicate 1 and 23% from Replicate 2 had no increase in MIC of colistin (Fig. S1 (b)). One explanation for this is the thick biofilms that were seen inside the bioreactors during adaptation, shown in our previous work (16). One asset of the continuous evolution bioreactors used in these studies is that they favor the formation of biofilms and can mimic some of the complex ecological environments that are not replicated in flask transfer based experimental

evolution where planktonic strains are favored. Thus, the selection environment could have favored not only drivers of colistin resistance but also those alleles that led to formation of complex biofilm communities. For example, while PmrA and B were known to be drivers for colistin resistance, proteins like PslA and MvfR that are involved in biofilm formation and quorum sensing were also prominent alleles reaching high frequencies in the evolving populations (17, 18). Biofilms are strongly associated with acute as well as chronic *P. aeruginosa* infections (19–21) and are also notorious for being tolerant to antimicrobial agents (19). Colistin resistance in biofilms has been attributed to induction of the *arn* operon (involved in lipopolysaccharide modification) in the metabolically active subpopulation of biofilms (22). Also, extracellular DNA in the biofilm matrix chelates positively charged magnesium ions creating a localized cation-limited environment leading to induction of the lipopolysaccharide (LPS) modification operon (23). These inducible mechanisms of colistin resistance could explain the observation of non-resistant end point isolates that survived in the bioreactor at high concentrations of colistin, presumably by being associated with the biofilm. Thus, while the role of alleles like *pslA* or *mvfR* may be in biofilm formation, they can indirectly play a role in imparting colistin non-susceptibility via enhancement of biofilm formation.

Also noteworthy was that 4 of the 29 sequenced end point isolates that were colistin susceptible had not acquired *mutS* mutations. Since hypermutation provides an adaptive advantage to evolve colistin resistance, protection from exposure to colistin by biofilms might make it possible for these non-hypermutating and non-adapted cells to persist within the bioreactor.

Biofilm formation by end point isolates was tested in microtiter plates using crystal violet staining (24) but a significant relationship could not be established between the MIC of the

isolates and their biofilm forming capacity (Fig. S6). However, this does not rule out the role of biofilms in providing protection against the drug within the bioreactor. While the design of the bioreactor used in this work promotes biofilm formation (16) there is no direct way of studying the dynamics of the developing biofilm community within the vessel during adaptation. Cells in the bioreactor are constantly adhering to and dissociating from the surfaces of the bioreactor, making it difficult to distinguish planktonic cells from biofilm associated cells at the end of the experiment. Furthermore, biofilm formation is a group behavior and one of the factors controlling it is quorum sensing (25). An individual end point isolate grown as a pure culture outside of the bioreactor does not experience the same environment and signals as it would inside the bioreactor vessel during adaptation and thus, may not exhibit the same group behavior as it would inside the vessel.

Predicted role of additional genes in resistance based on their known function

In addition to adaptive genes identified using statistic and phylogenetic strategies, genes mutated in some end point isolates could be associated with colistin resistance based on their known functions. Colistin resistance can be achieved by LPS modification and mutations were observed in genes modifying each component of the LPS: *arnT,* involved in addition of positively charged aminoarabinose to lipid A (26), *waaG*, involved in the synthesis of the LPS core (27), *wzz*, an O-antigen chain length regulator (28), *PA4517* or *cptA,* involved in addition of positively charged phosphoethanolamine to inner oligosaccharide core (29) and *PA3242,* involved in secondary acylation of lipid A (30). The role of these genes in resistance is purely speculative. Additionally, mutations in the outer membrane lipoprotein encoded by *blc,* which is upregulated in the absence

of the antimicrobial peptide sensor PhoQ (31) and efflux pumps and transporters, that are known to play a role in drug resistance (32, 33) can be implicated in colistin resistance.

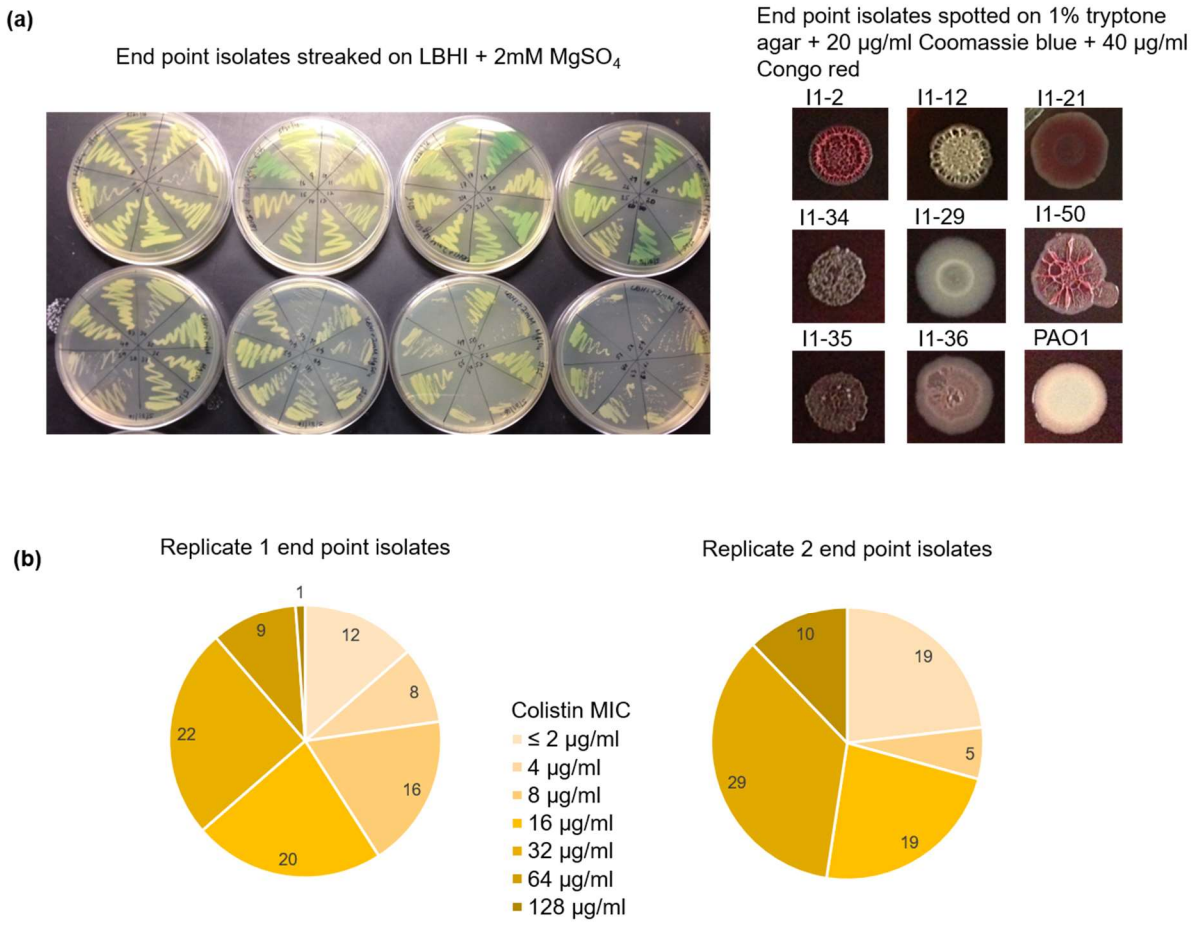

Figure S1. Phenotypic diversity of end point isolates obtained at the end of adaptation of PAO1 to colistin. (a) End point isolates showed variations in the size, color and texture when streaked on non-selective media (LBHI + 2mM $MgSO_4$). Spotting isolates on 1% tryptone agar supplemented with 20 µg/ml Coomassie blue and 40 µg/ml Congo red allowed the variations in morphology to become more apparent (21). Selected isolates are shown here. (b) Pie chart showing colistin minimum inhibitory concentrations (MICs) of end point isolates. Numbers in each segment represent the actual number of isolates from that population having the specific

colistin MIC as indicated by the colors in the legend. 12 out of 88 isolates from Replicate 1 (14%) and 19 out of the 82 isolates from Replicate 2 (23%) were colistin susceptible (MIC $\leq$ 2 µg/ml).

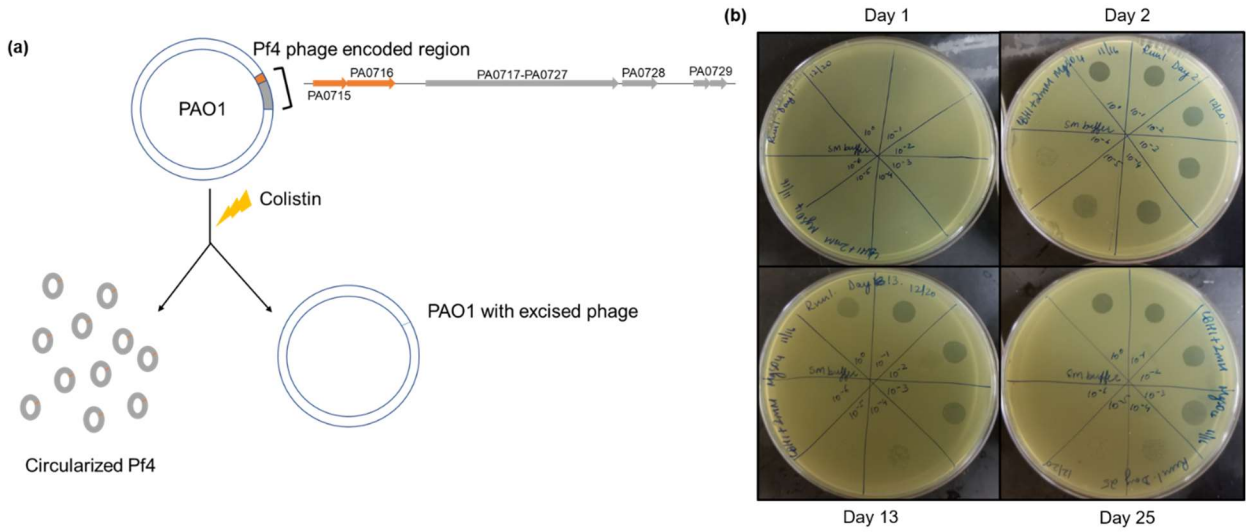

Figure S2. (a) Excision and circularization of phage Pf4 upon colistin exposure. The prophage, Pf4 exists in lysogenic state in PAO1. During exposure to colistin, the phage encoded DNA excised from the PAO1 chromosome and formed superinfective phage. (b) Induction of prophage during evolution of PAO1 to colistin. Top left panel shows different dilutions of the supernatant from day 1 of evolution (before drug exposure) that are incapable of lysing the lawn of PAO1 on the plate. The supernatant obtained after centrifugation of the population sample was filter sterilized and then serially diluted (10-fold dilutions) in SM buffer (50 mM Tris-HCl, pH 7.5 + 100 mM NaCl + 10 mM $MgSO_4.7H_2O$). 5 µl of each dilution was spotted on a lawn of PAO1. Supernatant from day 2 (first instance of drug exposure) has strong lytic activity (top right) suggesting induction of prophage and lytic capability. This lytic capability continues to

exist till the end of adaptation (bottom panels -days 13 and 25). All these samples are from Replicate 1 of adaptation that lasted 26 days.

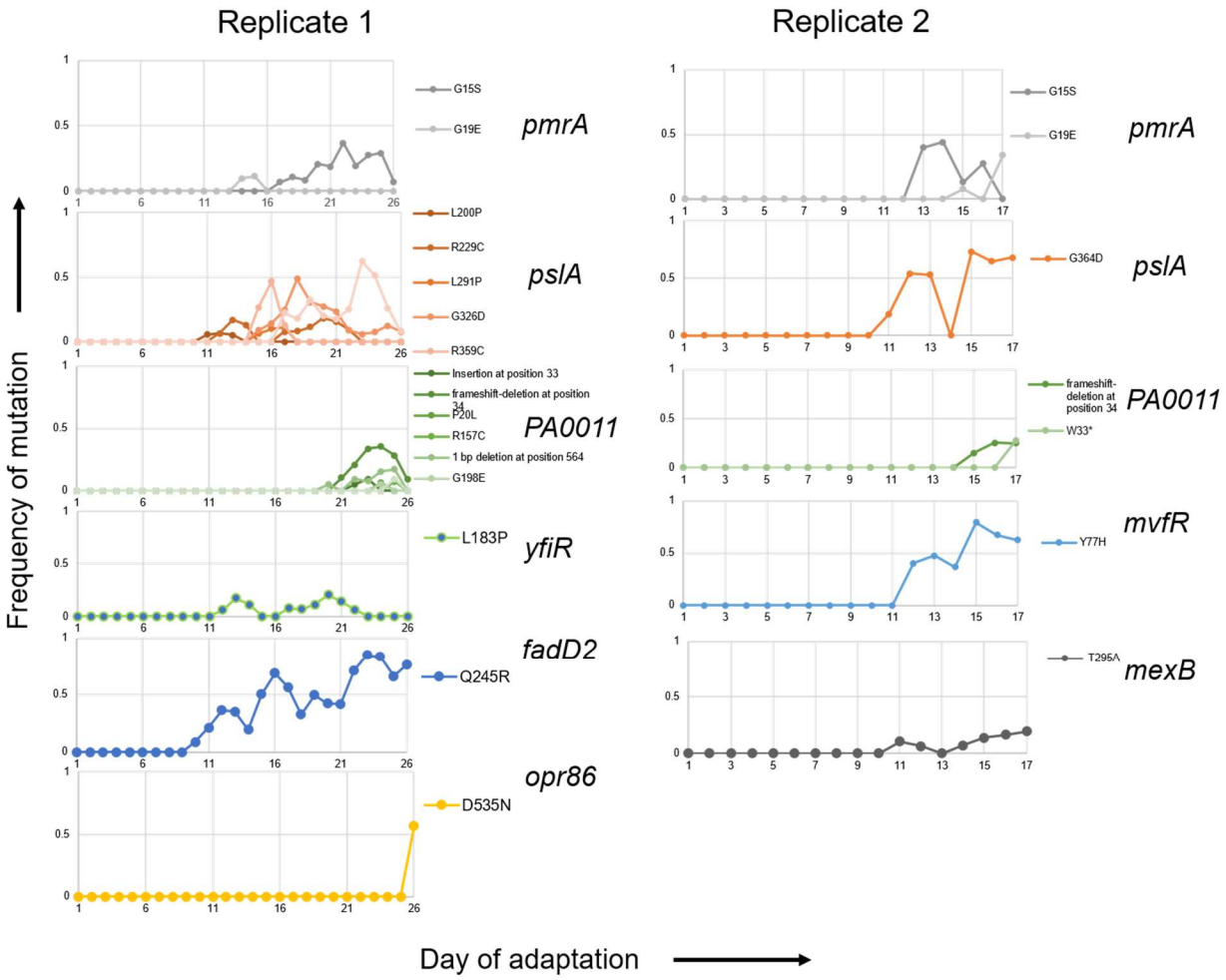

Figure S3. Evolutionary trajectories of adaptive mutations identified in this study. Each graph is a plot of the frequency of a mutation in a gene within the population versus the day of adaptation on which it was observed. Multiple mutations within a gene are plotted on the same graph using different colors to represent each mutation. Only alleles that rose above 10% frequency during adaptation are shown here. Evolutionary trajectories of the adaptive alleles of *pmrB* are shown in Figure S4.

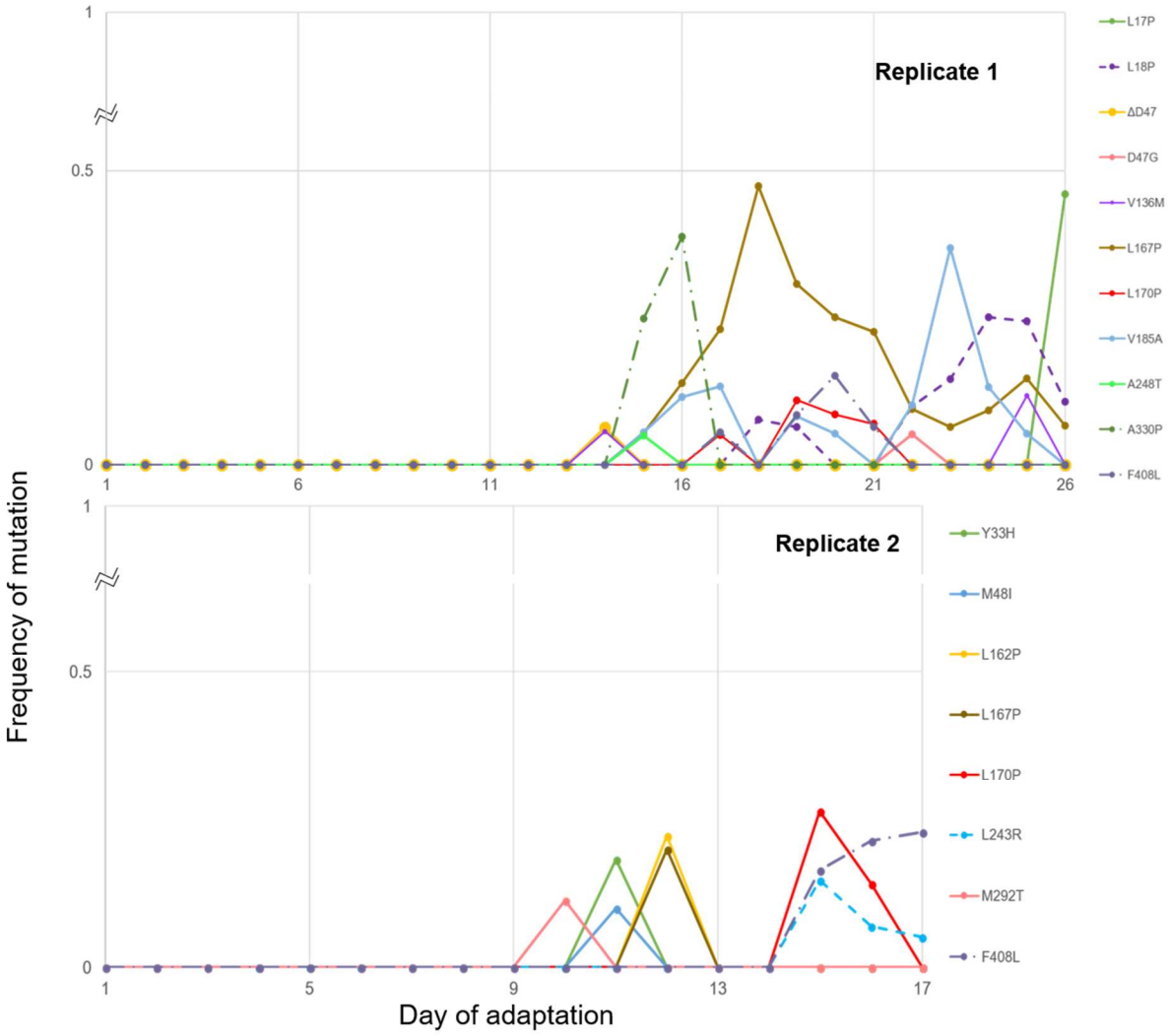

Figure S4. Trajectories of *pmrB* mutations detected at ≥ 5% frequency during adaptation to colistin. 11 mutations were identified in Replicate 1 which lasted 26 days. Out of the 11, only 3 mutations, L17P, L18P and L167P were detected in the final resistant population at ≥ 5% frequency. Replicate 2 which lasted 17 days had 8 *pmrB* mutations in the evolving population with only 2 mutations, L243R and F408L detectable in the final resistant population.

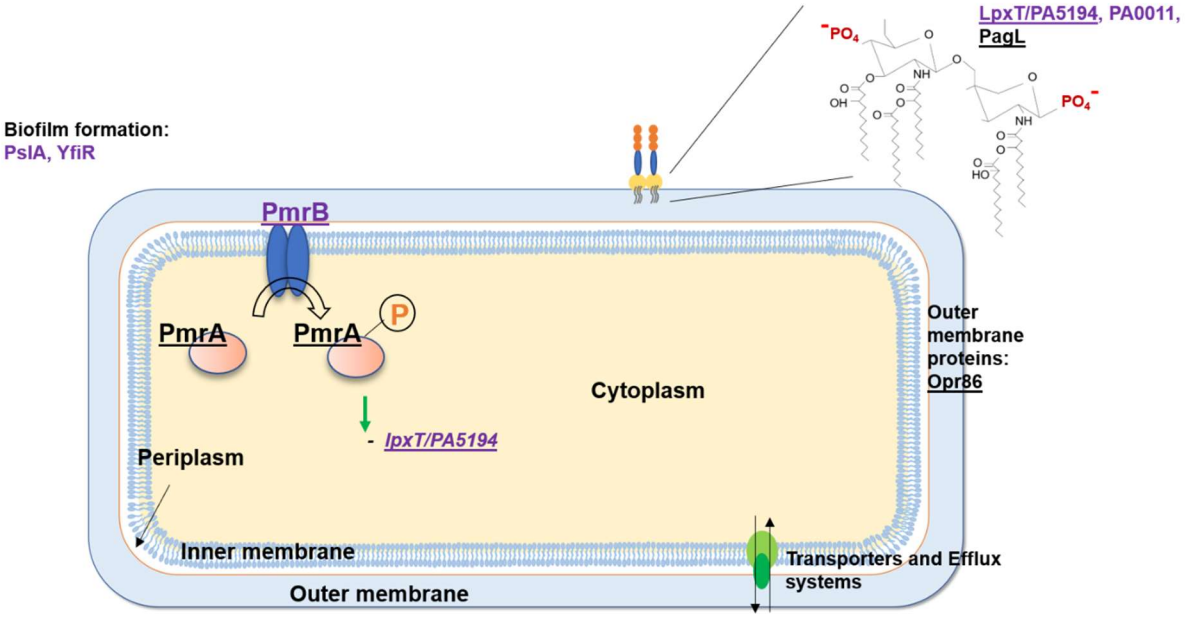

Figure S5. Cellular localization of targets identified in this study playing putative roles in colistin resistance. Targets in purple text were identified by the Fisher's Exact test of end point isolates and targets underlined were common among our study and other polymyxin resistance studies.

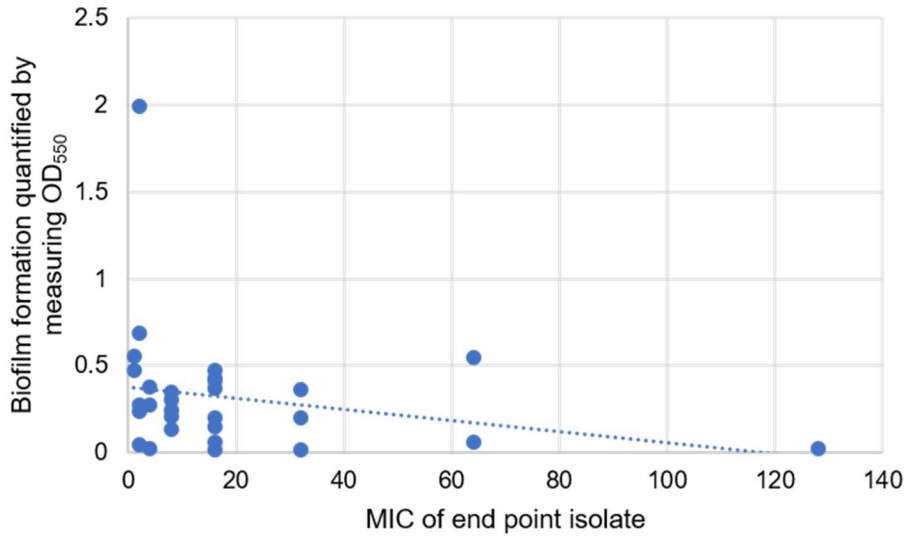

Figure S6. Relationship between colistin MIC of an end point isolate (in µg/ml) and its biofilm forming capability as measured by crystal violet staining. No significant co-relation between level of resistance of the isolate and its biofilm forming capability can be inferred from this data.

Table S1. List of end point isolates selected for whole genome sequencing and their minimum inhibitory concentrations (MICs) to colistin

MIC (µg/ml colistin)	Number of isolates with this MIC	Isolate number
1-2		PAO1 ancestor
1	1	I2-79
2	6	I1-2, I1-16, I1-50, I1-6, I1-76, I2-25
4	2	I1-21, I1-25,
8	5	I2-9, I2-26, I2-35, I2-38, I2-71
16	9	I1-39, I1-85, I1-53, I1-58, I1-62, I2-3, I2-46, I2-53, I2-55
32	3	I1-35, I2-58, I2-50
64	2	I1-36, I2-72
128	1	I1-37

MIC = Minimum Inhibitory Concentration
Nomenclature for isolate number: I=isolate; Number following I=bioreactor run from which clone was isolated; number following dash=number given to isolate

Table S2. Hypothetical protein encoding genes identified as significant by Fisher's Exact Test performed on mutations in daily populations of PAO1 evolving to colistin

Gene	Number of mutation events	Function	*p*-value	Comments
PA1232	8	Hypothetical protein	3.72E-06	
PA4452	4	Conserved hypothetical protein	1.15E-05	
PA5532	5	Hypothetical protein	2.26E-05	
PA4476	9	Hypothetical protein	5.20E-05	
PA4541	9	Hypothetical protein	1.14E-04	Mutation in PA4541 also identified in (34)
PA4991	5	Hypothetical protein	1.73E-04	
PA5391	4	Hypothetical protein	2.27E-04	
PA3307	3	Hypothetical protein	3.47E-04	
PA1624	4	Hypothetical protein	4.42E-04	
PA0095	6	Conserved hypothetical protein	4.47E-04	
PA3086	4	Hypothetical protein	5.62E-04	
PA4625	10	Hypothetical protein	5.73E-04	
PA1263	4	Hypothetical protein	7.92E-04	
PA5466	4	Hypothetical protein	7.92E-04	

References

1. Deatherage DE, Barrick JE. 2014. Identification of mutations in laboratory evolved microbes from next-generation sequencing data using breseq. Methods Mol Biol 1151:165–188.

2. Rice SA, Tan CH, Mikkelsen PJ, Kung V, Woo J, Tay M, Hauser A, Mcdougald D, Webb JS, Kjelleberg S. 2009. The biofilm life cycle and virulence of *Pseudomonas aeruginosa* are dependent on a filamentous prophage. ISME Hournal 3:271–282.

3. Mcelroy KE, Hui JGK, Woo JKK, Luk AWS, Webb JS, Kjelleberg S, Rice SA, Thomas T. 2014. Strain-specific parallel evolution drives short-term diversification during

Pseudomonas aeruginosa biofilm formation. Proc Natl Acad Sci 111:E1419–E1427.

4. Goerke C, Koller J, Wolz C. 2006. Ciprofloxacin and Trimethoprim Cause Phage Induction and Virulence Modulation in *Staphylococcus aureus.* Antimicrob Agents Chemother 50:171–177.

5. Hui JGK, Mai-prochnow A, Kjelleberg S, Mcdougald D, Rice SA. 2014. Environmental cues and genes involved in establishment of the superinfective Pf4 phage of *Pseudomonas aeruginosa*. Front Microbiol 5:654.

6. Nanda AM, Thormann K, Frunzke J. 2015. Impact of Spontaneous Prophage Induction on the Fitness of Bacterial Populations and Host-Microbe Interactions. J Bacteriol 197:410–419.

7. Webb JS, Thompson LS, James S, Charlton T, Tolker-nielsen T, Koch B, Givskov M, Kjelleberg S. 2003. Cell Death in *Pseudomonas aeruginosa* Biofilm Development. J Bacteriol 185:4585–4592.

8. Kim MK, Kang YK. 1999. Positional preference of proline in α-helices. Protein Sci 8:1492–1499.

9. Yun RH, Anderson A, Hermans J. 1991. Proline in a-Helix : Stability and Conformation Studied by Dynamics Simulation. Proteins Struct Funct Genet 10:219–228.

10. Moskowitz SM, Brannon MK, Dasgupta N, Pier M, Sgambati N, Miller AK, Selgrade SE, Miller SI, Denton M, Conway SP, Johansen HK, Høiby N. 2012. PmrB mutations promote polymyxin resistance of *Pseudomonas aeruginosa* isolated from colistin-treated cystic fibrosis patients. Antimicrob Agents Chemother 56:1019–1030.

11. Han M, Zhu Y, Creek DJ, Lin Y, Anderson D, Shen H, Tsuji B, Gutu AD, Moskowitz SM, Velkov T, Li J. 2018. Alterations of metabolic and lipid profiles in polymyxin-resistant *Pseudomonas aeruginosa*. Antimicrob Agents Chemother 62:e02656-17.

12. McPhee JB, Lewenza S, Hancock REW. 2003. Cationic antimicrobial peptides activate a two-component regulatory system, PmrA-PmrB, that regulates resistance to polymyxin B and cationic antimicrobial peptides in *Pseudomonas aeruginosa*. Mol Microbiol 50:205–217.

13. Lee JY, Park YK, Chung ES, Na IY, Ko KS. 2016. Evolved resistance to colistin and its loss due to genetic reversion in *Pseudomonas aeruginosa.* Sci Rep 6:25543.

14. Saxer G, Krepps MD, Merkley ED, Ansong C, Kaiser BLD, Valovska M-T, Ristic N, Yeh PT, Prakash VP, Leiser OP, Nakhleh L, Gibbons HS, Kreuzer HW, Shamoo Y. 2014. Mutations in global regulators lead to metabolic selection during adaptation to complex environments. PLOS Genet 10:e1004872.

15. Walkiewicz K, Benitez AS, Sun C, Bacorn C, Saxer G, Shamoo Y. 2012. Small changes in enzyme function can lead to surprisingly large fitness effects during adaptive evolution of antibiotic resistance. Proc Natl Acad Sci 109:21408–21413.

16. Mehta HH, Prater AG, Shamoo Y. 2018. Using experimental evolution to identify druggable targets that could inhibit the evolution of antimicrobial resistance. J Antibiot (Tokyo) 71:279–286.

17. Billings N, Millan MR, Caldara M, Rusconi R, Tarasova Y, Stocker R, Ribbeck K. 2013. The extracellular matrix component Psl provides fast- acting antibiotic defense in *Pseudomonas aeruginosa* biofilms. PLoS Pathog 9:e1003526.

18. Déziel E, Gopalan S, Tampakaki AP, Lépine F, Padfield KE, Saucier M, Xiao G, Rahme LG. 2005. The contribution of MvfR to *Pseudomonas aeruginosa* pathogenesis and quorum sensing circuitry regulation : multiple quorum sensing-regulated genes are modulated without affecting *lasRI , rhlRI* or the production of N-acyl-L-homoserine lactones. Mol Microbiol 55:998–1014.

19. Rybtke M, Hultqvist LD, Givskov M, Tolker-nielsen T. 2015. *Pseudomonas aeruginosa* biofilm infections : Community structure , antimicrobial tolerance and immune response. J Mol Biol 427:3628–3645.

20. Schaber JA, Triffo WJ, Suh SJ, Oliver JW, Hastert MC, Griswold JA, Auer M, Hamood AN, Rumbaugh KP. 2007. *Pseudomonas aeruginosa* forms biofilms in acute infection independent of cell-to-cell signaling. Infect Immun 75:3715–3721.

21. Flynn KM, Dowell G, Johnson TM, Koestler BJ, Waters CM, Cooper VS. 2016. Evolution of ecological diversity in biofilms of *Pseudomonas aeruginosa* by altered cyclic diguanylate signaling. J Bacteriol 198:2608–2618.

22. Pamp SJ, Gjermansen M, Johansen HK, Tolker-Nielsen T. 2008. Tolerance to the antimicrobial peptide colistin in *Pseudomonas aeruginosa* biofilms is linked to metabolically active cells , and depends on the *pmr* and *mexAB-oprM* genes. Mol Microbiol 68:223–240.

23. Mulcahy H, Charron-Mazenod L, Lewenza S. 2008. Extracellular DNA chelates cations and induces antibiotic resistance in *Pseudomonas aeruginosa* biofilms. PLoS Pathog 4:e1000213.

24. O'Toole GA. 2011. Microtiter dish biofilm formation assay. J Vis Exp 10–11.

25. O'Loughlin CT, Miller LC, Siryaporn A, Drescher K, Semmelhack MF, Bassler BL. 2013. A quorum-sensing inhibitor blocks *Pseudomonas aeruginosa* virulence and bio film formation. Proc Natl Acad Sci 110:17981–17986.

26. Fernández L, Jenssen H, Bains M, Wiegand I, Gooderham WJ, Hancock REW. 2012. The two-component system CprRS senses cationic peptides and triggers adaptive resistance in *Pseudomonas aeruginosa* independently of ParRS. Antimicrob Agents Chemother 56:6212–6222.

27. Muheim C, Bakali A, Engström O, Wieslander Å, Daley DO, Widmalm G. 2016. Identification of a fragment-based scaffold that inhibits the glycosyltransferase WaaG from *Escherichia coli*. Antibiotics 5:10.

28. Woodward R, Yi W, Li L, Zhao G, Eguchi H, Sridhar PR, Guo H, Song JK, Motari E, Cai L, Kelleher P, Liu X, Han W, Zhang W, Ding Y, Li M, Wang PG. 2010. In vitro bacterial polysaccharide biosynthesis: defining the functions of Wzy and Wzz. Nat Chem Biol 6:418–423.

29. Tamayo R, Choudhury B, Septer A, Merighi M, Carlson R, Gunn JS. 2005. Identification of *cptA* , a PmrA-regulated locus required for phosphoethanolamine modification of the *Salmonella enterica* serovar Typhimurium lipopolysaccharide core. J Bacteriol 187:3391–3399.

30. Liang Y, Guo Z, Gao L, Guo Q, Wang L, Han Y, Duan K, Shen L. 2016. The role of the temperature-regulated acyltransferase (PA3242) on growth, antibiotic resistance and virulence in *Pseudomonas aeruginosa*. Microb Pathog 101:126–135.

31. Gooderham WJ, Gellatly SL, Mcphee JB, Bains M, Cosseau C, Levesque RC, Hancock

REW. 2009. The sensor kinase PhoQ mediates virulence in *Pseudomonas aeruginosa*. Microbiology 155:699–711.

32. Yu Z, Qin W, Lin J, Fang S, Qiu J. 2015. Antibacterial mechanisms of polymyxin and bacterial resistance. Biomed Res Int 2015:article ID 679109, 11 pages.

33. Band V, Weiss D. 2015. Mechanisms of Antimicrobial Peptide Resistance in Gram-Negative Bacteria. Antibiotics 4:18–41.

34. Lee JY, Na IY, Park YK, Ko KS. 2014. Genomic variations between colistin-susceptible and -resistant *Pseudomonas aeruginosa* clinical isolates and their effects on colistin resistance. J Antimicrob Chemother 69:1248–1256.